

System-specific discrete variable representations for path integral calculations with quasi-adiabatic propagators

Maria Topaler and Nancy Makri

School of Chemical Sciences, University of Illinois, 505 S. Mathews Avenue, Urbana, IL 61801, USA

Received 21 May 1993

Discrete variable representations (DVRs), constructed numerically from eigenstates of the one-dimensional adiabatic potential, provide the optimal quadrature for evaluating quasi-adiabatic propagator path integrals (QUAPI) for a system coupled to a harmonic bath. Calculations of partition functions and reaction rates for a multiple-minimum potential in a dissipative environment illustrate the convergence characteristics of this approach. The small number of quadrature points required, along with the rapid convergence of QUAPI methods, results in a powerful numerical scheme, complementary to Monte Carlo methods, for performing condensed phase dynamics calculations over the entire temperature range of interest in chemical physics.

1. Introduction

In a series of recent papers [1–3], a new efficient path integral [4] methodology has been described for performing accurate quantum calculations on the real time dynamics of multidimensional Hamiltonians^{#1}. The basic advantage of that methodology arises from the use of improved reference Hamiltonians to split the time evolution operator. While a physically motivated partitioning of the Hamiltonian leads to propagators valid over large time steps (and therefore to rapid convergence of the discretized path integral), practical implementation requires use of numerical methods to generate these propagators. Provided that the zeroth-order system is decomposable into subsystems of sufficiently low dimensionality, which can be diagonalized numerically, the reference propagator can be obtained from the corresponding low-dimensional eigenstates. Specifically, the propagator for a one-dimensional reference subsystem with Hamiltonian $H(\hat{x}, \hat{p})$ can be expressed as [1],

$$\langle x'' | \exp(-i\hat{H}\Delta t/\hbar) | x' \rangle = \sum_{j=1}^M \Phi_j(x'') \Phi_j^*(x') \exp(-iE_j\Delta t/\hbar), \quad (1)$$

where x' and x'' are two arbitrary coordinate points, $(\hat{H} - E_j)\Phi_j = 0$ (Φ_1 is the ground state) and Δt is the time increment.

Numerical evaluation of eq. (1) is straightforward in imaginary time. In *real* time, though, the magnitude of successive terms in the above equation does not decrease with j . Indeed, the infinite number of terms that contribute to eq. (1) are responsible for the standard highly oscillatory behavior of the propagator. The key observation that allows propagators for arbitrary potentials to be constructed numerically according to eq. (1) is that terms involving eigenfunctions Φ_j that do not overlap with the wavefunction whose evolution is studied (j greater than some M_0) can be rigorously omitted without loss of accuracy [1,5,6]. This leads to *effective* propagators which can be obtained from eq. (1) with a finite number M of terms and which are *numerically exact* for the particular problem, provided that at least the lowest M_0 relevant basis functions are included

^{#1} For references to recent work on path integral methods for real time dynamics, see ref. [3].

($M \geq M_0$). Besides replacing an infinite sum by a finite one, this procedure has the additional advantage of filtering out rapidly oscillatory high energy contributions, thus leading to well-behaved propagators. In summary, therefore, the developed numerical propagator methodology offers two important advantages in the path integral: accurate dynamics with large time steps (i.e. few time slices), and relatively smooth integrand. The combination of these features allows efficient evaluation of the path integral for problems that appear extremely demanding if treated by other methods.

Although this approach is rather general, we have so far restricted ourselves to applications on problems that can be described by a system coupled to a harmonic bath. Apart from its importance to condensed phase chemistry and physics, a unique advantage offered by the system–bath model in the path integral context is the possibility of integrating out the bath analytically, leading to a reduced dimension path integral for the dynamics of the system with the effects of the bath described by a non-local influence functional [4,7]. The reduction in dimensionality is very desirable, as fewer integrations need to be performed numerically, but due to the introduction of non-local influence functional interactions the remaining integrals must be evaluated by global (i.e. non-iterative) methods.

We have found the adiabatic reference to provide a reasonable zeroth-order description of system bath problems, and constructed a *quasi-adiabatic propagator* [1]. The latter is comprised of a one-dimensional propagator which corresponds to the *exact* dynamics along the adiabatic path, and a displaced bath propagator which incorporates non-adiabatic corrections through Franck–Condon factors. Use of the quasi-adiabatic propagator in the discretized path integral with N time slices and elimination of the harmonic bath degrees of freedom leads to a path integral for the adiabatic reference system, with an influence functional that introduces multidimensional effects arising from the interaction with the bath. A number of calculations have shown that the quasi-adiabatic propagator path integral (QUAPI) requires a relatively small number of time slices. With typical parameters, the time evolution operator converges with five or six time steps for times of interest to chemical dynamics [1,2], and thus the path integral for the propagation of a wavefunction can be evaluated by ordinary quadratures (e.g., Simpson's rule). Condensed phase problems, though, require propagation of a density matrix, which involves evolution in forward and backward time, resulting in an integral of dimension $2N$, i.e. *double* that required for accurate discretization of a single time evolution operator. If the dynamics is sufficiently incoherent due to very strong friction or thermal averaging, we have found [3] that Monte Carlo evaluation of the QUAPI (modified to utilize the grid representation of the system propagators) yields accurate results with small statistical error. The more oscillatory nature of the integrand in cases of weakly damped processes (such as zero temperature dynamics with small to moderate dissipation) necessitates use of non-statistical (i.e. quadrature) methods. However, evaluation of the $2N$ -dimensional integral for the time-dependent density matrix is in practice an impossible task for $N > 3$ if treated by ordinary quadratures, which require for convergence at least 30 to 50 grid points per dimension.

The purpose of this Letter is to propose an optimal quadrature scheme for the evaluation of the path integral, which leads to dramatic savings and yields fully converged results free of statistical error. The idea is to use system-specific discrete variable representations (DVRs) [8–13], chosen to diagonalize the system position operator in the space of the eigenstates of the renormalized system Hamiltonian, in order to define a grid for the evaluation of the QUAPI. The number of DVR grid points required is equal to or slightly larger than the minimum number M_0 of states required for the system propagator and is generally fairly small, allowing efficient evaluation of the path integral with considerably larger numbers of time slices.

Section 2 reviews the QUAPI approach and describes the implementation of DVR quadratures. Section 3 presents applications of this scheme to compute partition functions and reaction rate constants for a model multiple-minimum potential over a wide range of temperatures. Finally, section 4 concludes with general remarks concerning the utility and future applications of this methodology.

2. Quasi-adiabatic propagator path integral (QUAPI) and discrete variable representation (DVR) grid

In this Letter, we consider the generic system–bath Hamiltonian,

$$\hat{H} = \hat{H}_s + \hat{H}_Q - \sum_{j=1}^n f_j(\hat{s}) \hat{Q}_j. \quad (2a)$$

Here \hat{H}_s describes the anharmonic system,

$$\hat{H}_s = \frac{\hat{p}_s^2}{2m_s} + V_0(\hat{s}), \quad (2b)$$

and

$$\hat{H}_Q = \sum_{j=1}^n \hat{H}_j, \quad \hat{H}_j = \frac{\hat{P}_j^2}{2m_j} + \frac{1}{2} m_j \omega_j^2 \hat{Q}_j^2 \quad (2c)$$

is the Hamiltonian for the n harmonic oscillators $\{\hat{Q}_j\}$ which are linearly coupled to the system and which constitute the bath.

In order to construct an accurate propagator we partition the total Hamiltonian into a one-dimensional reference Hamiltonian H'_s with the potential along the adiabatic path,

$$H'_s(\hat{s}, \hat{p}_s) \equiv \frac{\hat{p}_s^2}{2m_s} + V_0(\hat{s}) - \sum_{j=1}^n \frac{f_j(\hat{s})^2}{2m_j \omega_j^2}, \quad (3a)$$

and a bath \hat{H}'_Q of n adiabatically displaced oscillators,

$$\hat{H}'_Q \equiv \sum_{j=1}^n H'_j(\hat{Q}_j, \hat{P}_j; \hat{s}) \equiv \sum_{j=1}^n \left[\frac{\hat{P}_j^2}{2m_j} + \frac{1}{2} m_j \omega_j^2 \left(\hat{Q}_j - \frac{f_j(\hat{s})}{m_j \omega_j^2} \right)^2 \right]. \quad (3b)$$

Employing a symmetric splitting of the short-time evolution operator,

$$\exp(-i\hat{H}\Delta t/\hbar) \approx \exp(-i\hat{H}'_Q \Delta t/2\hbar) \exp(-i\hat{H}'_s \Delta t/\hbar) \exp(-i\hat{H}'_Q \Delta t/2\hbar), \quad (4)$$

leads to the following *quasi-adiabatic propagator* [1]:

$$\begin{aligned} \langle s_k \mathbf{Q}_k | \exp(-i\hat{H}\Delta t/\hbar) | s_{k-1} \mathbf{Q}_{k-1} \rangle &\approx \langle s_k | \exp(-i\hat{H}'_s \Delta t/\hbar) | s_{k-1} \rangle \\ &\times \prod_{j=1}^n \langle Q_{j,k} | \exp[-i\hat{H}'_j(s_k) \Delta t/2\hbar] \exp[-i\hat{H}'_j(s_{k-1}) \Delta t/2\hbar] | Q_{j,k-1} \rangle, \end{aligned} \quad (5)$$

where the coordinate points have been labeled by the integers $k-1$ and k in anticipation of the discretized path integral expression, eq. (7) below.

Each bath factor in the last equation is a propagator for a harmonic oscillator displaced (symmetrically) from equilibrium by amounts that depend on the value of the system coordinate. These propagators can be evaluated analytically, introducing Franck–Condon factors [1] that account for non-adiabatic corrections to the dynamics along the one-dimensional adiabatic path. The one-dimensional system propagators are constructed numerically, as described in section 1, in terms of M system eigenstates Φ_j and eigenvalues E_j of \hat{H}'_s :

$$\langle s_k | \exp(-i\hat{H}'_s \Delta t/\hbar) | s_{k-1} \rangle = \sum_{j=1}^M \Phi_j(s_{k-1}) \Phi_j(s_k) \exp(-iE_j \Delta t/\hbar). \quad (6)$$

This propagator matrix is generated at the beginning of the calculation and stored on the chosen grid.

Use of eq. (5) leads to discretized path integral expressions for the dynamical quantities of interest; for ex-

ample, the propagator between the coordinate points $s_0\mathbf{Q}_0$ and $s_N\mathbf{Q}_N$ takes the form

$$\langle s_N\mathbf{Q}_N | \exp(-i\hat{H}t/\hbar) | s_0\mathbf{Q}_0 \rangle = \int_{-\infty}^{\infty} ds_1 \dots \int_{-\infty}^{\infty} ds_N \prod_{k=1}^N \langle s_k | \exp(-i\hat{H}'_s \Delta t/\hbar) | s_{k-1} \rangle \\ \times I(s_0, s_1, \dots, s_N; \mathbf{Q}_0, \mathbf{Q}_N), \quad (7a)$$

where

$$I(s_0, s_1, \dots, s_N; \mathbf{Q}_0, \mathbf{Q}_N) = \prod_{j=1}^n I_j(s_0, s_1, \dots, s_N; \mathbf{Q}_0, \mathbf{Q}_N), \quad (7b)$$

$$I_j = \langle \mathbf{Q}_{j,N} | \exp[-i\hat{H}'_j(s_N)\Delta t/2\hbar] \exp[-i\hat{H}'_j(s_{N-1})\Delta t/\hbar] \dots \\ \times \exp[-i\hat{H}'_j(s_1)\Delta t/\hbar] \exp[-i\hat{H}'_j(s_0)\Delta t/2\hbar] | \mathbf{Q}_{j,0} \rangle \quad (7c)$$

is an influence functional which incorporates multidimensional non-adiabatic corrections to the *exact* dynamics along the adiabatic path described by the one-dimensional system propagators of eq. (7a). Application of the same procedure to calculate probabilities averaged over the bath, such as the canonical density matrix, results in similar path integral expressions but with $2N$ (rather than $N-1$) integrations and properly averaged influence functionals. In all cases the influence functional is given by the expressions obtained by Feynman and Vernon [9], but the force $f_j(t') \equiv f_j(s(t'))$ exerted on the bath by the system is in the present formulation constant during time lengths over which the system coordinate s_k is fixed [3], changing discontinuously as the value of the system coordinate is changed from s_k to s_{k+1} .

The main focus of this Letter is on the numerical evaluation of eq. (7) (or similar properly averaged QUAPI expressions). As noted in section 1, integration using Monte Carlo algorithms is not possible, unless the system propagators and/or the influence functional contain sufficiently strong damping factors. Thus, we seek efficient quadrature schemes that require small numbers of points per dimension which should be practical for evaluating the multidimensional discretized path integral.

Clearly, much more efficient than the coordinate representation would be to use bound basis functions to discretize the path integral. The adiabatic system propagator is *diagonal* in the basis of eigenstates of \hat{H}'_s , and a small number (typically, 10–20) of such basis functions should provide an adequate representation of the influence functional. In contrast, discretization in coordinate space requires a larger number of grid points (typically, 30–100). However, potential coupling terms are not local in the eigenstate basis, and this necessitates use of the coordinate representation in order to obtain influence functionals that factorize as in eq. (7b).

Therefore, the question that arises is whether one can find a discrete basis that requires for completeness the same (small) number of terms as the eigenstate basis, but which also diagonalizes the potential coupling. Such basis sets, known as discrete variable representations [8–11,14], were introduced many years ago as convenient schemes for evaluating potential matrix elements [8,9]. In the last decade, Light and co-workers extended the DVR ideas to develop powerful methods for treating vibrational eigenvalue problems [10,11]. Uniform grid discrete variable representations of the kinetic energy matrix and of the free particle propagator have been utilized recently in reactive scattering calculations [12]. DVR grids have also been combined with Fourier grids in iterative wavepacket propagation algorithms [13,15]. In this work we adopt a (non-Gaussian in general) system-specific DVR quadrature, similar to the potential optimized DVR of Echave and Clary [14], in order to evaluate the multidimensional integral that appears in QUAPI expressions. In the present case the DVR grid is one-dimensional and is constructed from the exact eigenstates of the renormalized system Hamiltonian.

The DVR basis is constructed by performing a unitary transformation on the basis $\{\Phi_i\}$ of the M lowest energy eigenstates of H'_s ,

$$|u_i\rangle = \sum_{i'=1}^M L_{ii'} |\Phi_{i'}\rangle. \quad (8a)$$

(The choice of basis size M will be discussed later in this section.) The DVR states $\{|u_i\rangle\}$ are further specified by the requirement that the system position operator \hat{s} be diagonal in the new basis,

$$\langle u_i | \hat{s} | u_{i'} \rangle = s_i^{\text{DVR}} \delta_{ii'}. \quad (8b)$$

The DVR states $|u_i\rangle$ are the discrete analog of the ordinary coordinate eigenstates, and the eigenvalues s_i^{DVR} , $i=1, \dots, M$ form the DVR grid. The fact that the $|u_i\rangle$ basis is nothing but a rotation of the eigenstate basis implies that the DVR grid may be quite sparse; yet, the potential operator is diagonal, leading to appealing expressions.

Discretization of the path integral in the DVR basis and repeated use of the standard spectral expansion for the displaced bath time-evolution operator,

$$\exp[-iH_j(\hat{Q}_j, \hat{P}_j; \hat{s})] = \sum_{i=1}^M |u_i\rangle \exp[-iH_j(\hat{Q}_j, \hat{P}_j; s_i^{\text{DVR}})] \langle u_i| \quad (9)$$

leads to the following DVR representation of the QUAPI for the coordinate propagator:

$$\begin{aligned} \langle s_N \mathbf{Q}_N | \exp(-i\hat{H}t/\hbar) | s_0 \mathbf{Q}_0 \rangle &= \sum_{i_1=1}^M \dots \sum_{i_{N-1}=1}^M \langle s_N | \exp(-i\hat{H}'_s \Delta t/\hbar) | u_{i_{N-1}} \rangle \prod_{k=2}^{N-1} \langle u_{i_k} | \exp(-i\hat{H}'_s \Delta t/\hbar) | u_{i_{k-1}} \rangle \\ &\times \langle u_{i_1} | \exp(-i\hat{H}'_s \Delta t/\hbar) | s_0 \rangle I(s_0 s_{i_1}^{\text{DVR}}, \dots, s_{i_{N-1}}^{\text{DVR}}, s_N; \mathbf{Q}_0, \mathbf{Q}_N). \end{aligned} \quad (10)$$

Eq. (10) is the DVR analog of eq. (7). The expression for the influence functional is unchanged but is now evaluated at the specific DVR points. The DVR representation of the one-dimensional propagator for the adiabatic system Hamiltonian is constructed numerically with the aid of the basis transformation relations, eq. (8).

In the absence of system-bath coupling, the number M of terms required in eq. (10) would be *exactly* equal to the minimum number M_0 of terms required to represent the system propagator. For non-zero coupling, though, the spectral expansion of eq. (9) requires an adequate number M of terms for completeness, which may be larger than M_0 . Numerical calculations, some of which are presented in section 3, show that the number M of DVR points required for convergence is typically slightly larger than the number M_0 of states required to expand the system propagator. For low-lying bound states or low-temperature processes, we find that approximately 4–10 DVR points are sufficient, compared to 30–50 quadrature points that would be necessary if a non-optimal grid were used. Thus, the enormous acceleration of QUAPI calculations achievable with the DVR grid is apparent, particularly if the number of integrations to be performed is large.

3. Application: reaction rates in the condensed phase

To demonstrate the advantages of adopting optimal DVR grids in the evaluation of the path integral we present in this section numerical applications on condensed phase reaction rate constants. Condensed phase environments are usually described well by harmonic baths and the QUAPI methodology is ideally suited. An efficient fully quantum-mechanical scheme for calculating Boltzmann averaged rate constants based on Miller's flux correlation function formalism [16] has been described in a recent paper [3]. Here we review the basic formalism and present numerical results on a model Hamiltonian.

The thermal rate coefficient is given by the time integral of the flux-flux correlation function [16],

$$k = Z^{-1} \int_0^{t_p} C_f(t) dt, \quad (11)$$

where Z denotes the canonical partition function of the reactants, t_p is the conventional "plateau time" [17] and the correlation function is defined by

$$C_f(t) = \text{Tr}[\hat{F} \exp(i\hat{H}t_c^*/\hbar) \hat{F} \exp(-i\hat{H}t_c/\hbar)]. \quad (12)$$

Here \hat{F} is the symmetrized flux operator

$$\hat{F} = \frac{1}{2m_s} [\hat{p}_s \delta(\hat{s}) + \delta(\hat{s}) \hat{p}_s], \quad (13)$$

and the "dividing surface" through which the reactive flux is measured is located for notational simplicity at $s=0$; $t_c = t - \frac{1}{2}i\hbar\beta$ is a complex time that arises from combining the time evolution operator with the Boltzmann operator and $\beta = 1/k_B T$. Evaluating eq. (12) in coordinate space and calculating derivatives by finite difference leads [3] to the following expression for the correlation function:

$$C_f(t) = \frac{\hbar^2}{2m_s^2 s_{FD}^2} \text{Re}[K(s_{FD}, s_{FD}, 0, 0; t_c) - K(0, s_{FD}, 0, s_{FD}; t_c)], \quad (14)$$

where s_{FD} is a coordinate point sufficiently close to the dividing surface and

$$K(s_0, s_N, s_{N+1}, s_{2N+1}; t_c) \equiv \int_{-\infty}^{\infty} d^n \mathcal{Q}_0 \langle \mathcal{Q}_0 | \langle s_{2N+1} | \exp(i\hat{H}t_c^*/\hbar) | s_{N+1} \rangle \langle s_N | \exp(-i\hat{H}t_c/\hbar) | s_0 \rangle | \mathcal{Q}_0 \rangle. \quad (15)$$

If the propagators in the last equation are expressed in the QUAPI form one arrives at the result

$$K(s_0, s_N, s_{N+1}, s_{2N+1}; t_c) = \int_{-\infty}^{\infty} ds_1 \dots \int_{-\infty}^{\infty} ds_{N-1} \int_{-\infty}^{\infty} ds_{N+2} \dots \int_{-\infty}^{\infty} ds_{2N} \prod_{k=N+1}^{2N+1} \langle s_k | \exp(i\hat{H}_s \Delta t_c^*/\hbar) | s_{k-1} \rangle \\ \times \prod_{k=1}^N \langle s_k | \exp(-i\hat{H}_s \Delta t_c/\hbar) | s_{k-1} \rangle I(s_0, s_1, \dots, s_{N-1}, s_N, s_{N+1}, \dots, s_{2N+1}), \quad (16)$$

which requires $2N-2$ numerical integrations. The influence functional I in eq. (16) is given by the expression

$$I = I^0 \prod_{j=1}^n \exp\left(-\frac{1}{m_j \omega_j^3 \hbar} \sum_{k=0}^{2N+1} \sum_{k'=0}^{2N+1} \alpha_{kk'}(\omega_j, \Delta t_c) f_j(s_k) f_j(s_{k'})\right), \quad (17)$$

where I^0 is the partition function for the uncoupled bath, the coefficients are given by the equations [3]

$$\alpha_{kk}(\omega_j, \Delta t_c) = \sin[\omega_j(t_{k+1} - t_k + i\hbar\beta)/2] \sin[\omega_j(t_{k+1} - t_k)/2] / \sinh(\hbar\omega_j\beta/2), \\ \alpha_{kk'}(\omega_j, \Delta t_c) = \cos[\omega_j(t_{k+1} + t_k - t_{k'+1} - t_{k'} + i\hbar\beta)/2] \sin[\omega_j(t_{k+1} - t_k)/2] \\ \times \sin[\omega_j(t_{k'+1} - t_{k'})/2] / \sinh(\hbar\omega_j\beta/2), \quad k > k' \quad (18)$$

and the discrete complex times t_k are defined such that the value of the system coordinate is s_k between t_k and t_{k+1} along the complex time contour implicit in eq. (16) (see figs. 1 and 2 of ref. [3]). If the coupling is bilinear,

$$f_j(\hat{s}) = c_j \hat{s}, \quad (19)$$

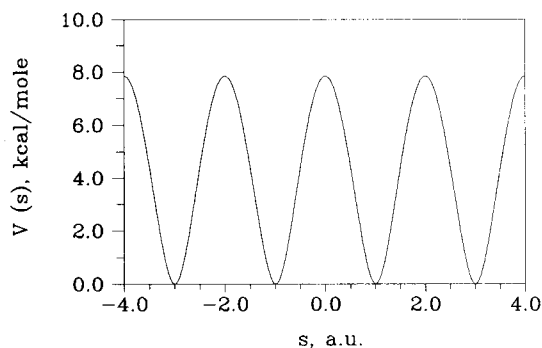


Fig. 1. The periodic potential used in the numerical calculations of section 3 along the adiabatic path, $V(s) = V_0(s) - \sum_j f_j(s)^2 / 2m_j\omega_j^2$. The one-period grid referred to in the text corresponds to the range $-2 < s < 2$, while the two-period grid involves $-4 < s < 4$ au.

and the bath is described by a continuous spectral density

$$J(\omega) = \frac{\pi}{2} \sum_j \frac{c_j^2}{m_j\omega_j} \delta(\omega - \omega_j), \quad (20)$$

we have shown [3] that the influence functional takes the form

$$I = I^0 \exp\left(-\frac{2}{\pi\hbar} \sum_{k=0}^{2N+1} \sum_{k'=0}^{2N+1} s_k s_{k'} \int d\omega \frac{J(\omega)}{\omega^2} \alpha_{kk'}(\omega, \Delta t_c)\right). \quad (21)$$

For the numerical calculations of this section we consider a periodic multiple minimum potential with barrier height approximately equal to 8 kcal/mol (see fig. 1) coupled linearly to a continuous bath with spectral density

$$J(\omega) = \eta\omega^3 \exp(-\omega/\omega_c), \quad (22)$$

with $\omega_c = 50 \text{ cm}^{-1}$ and $\eta = 10^8 \text{ au}$. The complex time propagators, eq. (16), as well as the partition function Z , are represented on the DVR grid introduced in section 2. A one-period grid was adequate at low temperature, while higher temperature calculations required a larger coordinate range^{#2} (see fig. 1). Results are presented for two temperatures corresponding to tunneling and activated kinetics, respectively.

Tables 1 and 2 show the convergence of the reactant partition function Z at $T = 100$ and 400 K as a function

^{#2} The calculations presented here, intended only as a convergence test of the proposed methodology, simply measure the rate of crossing the dividing surface at $s = 0$, which is *not* identical to the site-to-site hopping rate for the periodic potential at high temperature. Site-to-site and multiple site hopping rates can be obtained using modified flux correlation function expressions; see, for example, refs. [18,19].

Table 1
Reactant partition function for $T = 100$ K (one-period grid)

N	$M=4$	$M=6$	$M=8$	$M=12$
1	0.64604×10^{-4}	0.64604×10^{-4}	0.64604×10^{-4}	0.64604×10^{-4}
2	0.61429×10^{-4}	0.61510×10^{-4}	0.61494×10^{-4}	0.61494×10^{-4}
3	0.60322×10^{-4}	0.60423×10^{-4}	0.60402×10^{-4}	0.60402×10^{-4}
4	0.59762×10^{-4}	0.59857×10^{-4}	0.59836×10^{-4}	0.59835×10^{-4}
5	0.59440×10^{-4}	0.59523×10^{-4}	0.59502×10^{-4}	0.59501×10^{-4}
6	0.59239×10^{-4}	0.59311×10^{-4}	0.59291×10^{-4}	0.59290×10^{-4}
7	0.59107×10^{-4}	0.59170×10^{-4}	0.59150×10^{-4}	0.59149×10^{-4}
8	0.59016×10^{-4}	0.59071×10^{-4}	0.59052×10^{-4}	0.59051×10^{-4}
$\rightarrow \infty^a)$	0.58669×10^{-4}	0.58688×10^{-4}	0.58674×10^{-4}	0.58672×10^{-4}

^{a)} Richardson extrapolation.

Table 2
Reactant partition function for $T=400$ K (two-period grid)

N	$M=6$	$M=10$	$M=14$	$M=18$
1	0.90443×10^{-1}	0.91133×10^{-1}	0.91157×10^{-1}	0.91158×10^{-1}
2	0.89993×10^{-1}	0.90160×10^{-1}	0.90166×10^{-1}	0.90164×10^{-1}
3	0.89887×10^{-1}	0.89938×10^{-1}	0.89939×10^{-1}	0.89936×10^{-1}
4	0.89847×10^{-1}	0.89856×10^{-1}	0.89855×10^{-1}	0.89852×10^{-1}
5	0.89827×10^{-1}	0.89817×10^{-1}	0.89814×10^{-1}	0.89812×10^{-1}
6	0.89817×10^{-1}	0.89795×10^{-1}	0.89792×10^{-1}	0.89789×10^{-1}
$\rightarrow \infty$ ^{a)}	0.89795×10^{-1}	0.89749×10^{-1}	0.89732×10^{-1}	0.89740×10^{-1}

a) Richardson extrapolation.

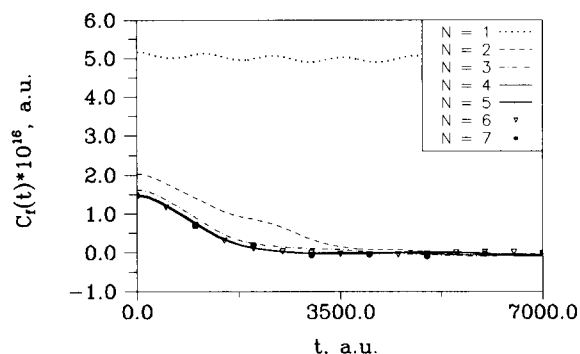


Fig. 2. The flux-flux correlation function for the periodic potential discussed in section 3 at $T=100$ K for various numbers of time slices N . The path integral was evaluated with the DVR quadrature described in section 2 with 6 DVR points for $N \leq 6$. Monte Carlo results with $N=7$ are also indicated by the circles for comparison.

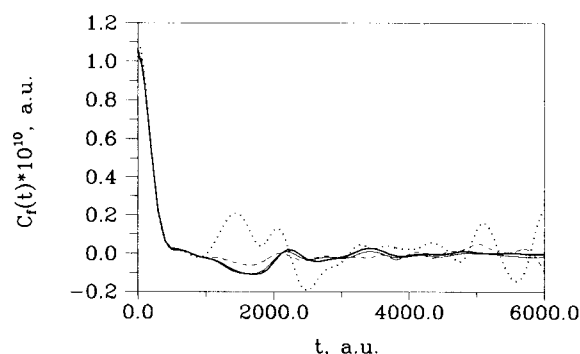


Fig. 3. The flux-flux correlation function for the periodic potential discussed in section 3 at $T=400$ K for various numbers of time slices N . The path integral was evaluated with the DVR quadrature described in section 2 with 18 DVR points. (\cdots) $N=1$; ($---$) $N=2$; ($---$) $N=3$; ($---$) $N=4$.

of the number N of time slices used to discretize the path integral and the number M of DVR points used to evaluate it. Convergence to about 2% is achieved with just four time slices at $T=100$ K, and very accurate results can be obtained [1] using Richardson extrapolation [20]. Table 1 also shows that a six-point DVR quadrature is exact for this low temperature. As seen from table 2, a larger number of DVR points must be used at higher temperatures ($M=10$ for $T=400$ K), but the path integral converges with fewer time slices (and therefore requires fewer integrations) as the temperature is increased. The combination of these features makes the DVR-QUAPI scheme extremely efficient both at high and low temperatures.

Figs. 2 and 3 illustrate similar convergence trends for the flux correlation function. Fig. 2 shows that the $N=4$ results are almost converged at $T=100$ K, while fully converged results are obtained with six time slices. Calculation of the flux correlation function requires evaluation of a ten-dimensional integral for $N=6$, and this can be performed *by quadrature* because just six DVR points per integration variable are sufficient in the deep tunneling regime.

The flux correlation function at $T=400$ K is shown in fig. 3. At this temperature, the system shows Arrhenius behavior and requires a grid of two potential periods (cf. fig. 1). The correlation function approaches its plateau value rather slowly in this case ($t_p \approx 6\hbar\beta$) exhibiting substantial recurrences [21]. A larger number of DVR points ($M=18$) are required to discretize the system coordinate in this case, but the QUAPI converges already at $N=3$, making numerical integration easily manageable.

All calculations reported in this section were performed on RISC 6000/350 workstations and required CPU time ranging from a few minutes to a few hours. Thus, it is seen that the use of the DVR allows accurate and efficient evaluation of the QUAPI both at high and low temperatures, providing a convenient alternative to Monte Carlo integration methods which (as discussed in section 1) are often not applicable.

4. Concluding remarks

We have explored an efficient quadrature scheme for evaluating discretized path integral expressions for systems interacting with harmonic oscillator environments. The combination of an improved quasi-adiabatic splitting of the time-evolution operator employed in the QUAPI with an optimal DVR quadrature for the system coordinate results in a very efficient scheme for studying the dynamics of condensed phase systems. The method is very easy to implement and converges rapidly, both with respect to the number of time slices in the path integral and to the number of DVR points, yielding reliable results free of Monte Carlo statistical error. This is particularly important for zero temperature (i.e. purely real time) calculations, which are characterized by delocalized oscillatory integrands and cannot be dealt with by statistical sampling methods. However, the rapid convergence and ease of implementation of the method make it attractive also for the calculation of partition functions or free energies, as well as of thermally averaged time correlation functions. In the latter case we expect combination of DVR and Monte Carlo schemes to provide powerful methods applicable over a wide range of parameters.

A number of applications of this methodology are in progress by our group and will be presented in future publications.

Acknowledgement

This work has been supported by the National Science Foundation under the Materials Research Laboratory Grant NSF-DMR 89-20538.

References

- [1] N. Makri, Chem. Phys. Letters 193 (1992) 435; in: Time-dependent quantum molecular dynamics, eds. J. Broeckhove and L. Lathouwers (Plenum Press, New York, 1992) p. 209.
- [2] M. Topaler and N. Makri, J. Chem. Phys. 97 (1992) 9001.
- [3] M. Topaler and N. Makri, Chem. Phys. Letters 210 (1993) 285.
- [4] R.P. Feynman, Rev. Mod. Phys. 20 (1948) 367;
R.P. Feynman and A.R. Hibbs, Quantum mechanics and path integrals (McGraw-Hill, New York, 1965).
- [5] N. Makri, Chem. Phys. Letters 159 (1989) 489.
- [6] N. Makri, J. Phys. Chem. 97 (1993) 2417.
- [7] R.P. Feynman and F.L. Vernon Jr., Ann. Phys. 24 (1963) 118.
- [8] D.O. Harris, G.G. Engerholm and W.D. Gwinn, J. Chem. Phys. 43 (1965) 1515.
- [9] A.S. Dickinson and P.R. Certain, J. Chem. Phys. 49 (1968) 4209.
- [10] J.V. Lill, G.A. Parker and J.C. Light, Chem. Phys. Letters 89 (1982) 483; J. Chem. Phys. 85 (1986) 900;
J.C. Light, I.P. Hamilton and J.V. Lill, J. Chem. Phys. 82 (1985) 1400.
- [11] S.E. Choi and J.C. Light, J. Chem. Phys. 92 (1990) 2129;
Z. Bačić and J.C. Light, J. Chem. Phys. 85 (1986) 4594; 86 (1987) 3065; Ann. Rev. Phys. Chem. 40 (1989) 469.
- [12] D.T. Colbert and W.H. Miller, J. Chem. Phys. 96 (1992) 1982;
S.M. Auerbach and W.H. Miller, J. Chem. Phys. 98 (1993) 6917.

- [13] M.R. Hermann and J.A. Fleck Jr., Phys. Rev. A 38 (1988) 6000;
F. Le Quere and C. Leforestier, J. Chem. Phys. 92 (1990) 247;
J.A. Bentley, R.E. Wyatt, M. Menou and C. Leforestier, J. Chem. Phys. 97 (1992) 4255.
- [14] J. Echave and D.C. Clary, Chem. Phys. Letters 190 (1992) 225.
- [15] S. Das and D.J. Tannor, J. Chem. Phys. 92 (1990) 3403;
C.J. Williams, J. Qian and D.J. Tannor, J. Chem. Phys. 95 (1991) 1721.
- [16] W.H. Miller, S.D. Schwartz and J.W. Tromp, J. Chem. Phys. 79 (1983) 4889.
- [17] D. Chandler, Introduction to modern statistical mechanics (Oxford Univ. Press, Oxford, 1987).
- [18] A.F. Voter and J.D. Doll, J. Chem. Phys. 82 (1985) 90.
- [19] G. Wahnstrom and H. Metiu, Chem. Phys. Letters 145 (1988) 44;
G. Wahnstrom, J. Chem. Phys. 89 (1988) 6996.
- [20] W.H. Press, B.P. Flannery, S.A. Teukolsky and W.T. Vetterling, Numerical recipes (Cambridge Univ. Press, Cambridge, 1989).
- [21] T.N. Truong, J.A. McCammon, D.J. Kouri and D.K. Hoffman, J. Chem. Phys. 96 (1992) 8136.